



Impairment of carotenoid biosynthesis through *CAR1* gene mutation results in CoQ₁₀, sterols, and phytoene accumulation in *Rhodotorula mucilaginosa*

Jana Tkáčová¹ · Giacomo Zara² · Giuseppe Ianiri³ · Raffaello Castoria³ · Milan Čertík¹ · Ilaria Mannazzu²

Received: 11 August 2021 / Revised: 26 October 2021 / Accepted: 28 October 2021 / Published online: 15 December 2021
© The Author(s), under exclusive licence to Springer-Verlag GmbH Germany, part of Springer Nature 2021

Abstract

Red yeasts, mainly included in the genera *Rhodotorula*, *Rhodospiridiobolus*, and *Sporobolomyces*, are renowned biocatalysts for the production of a wide range of secondary metabolites of commercial interest, among which lipids, carotenoids, and other isoprenoids. The production of all these compounds is tightly interrelated as they share acetyl-CoA and the mevalonate pathway as common intermediates. Here, T-DNA insertional mutagenesis was applied to the wild type strain C2.5t1 of *Rhodotorula mucilaginosa* for the isolation of albino mutants with impaired carotenoids biosynthesis. The rationale behind this approach was that a blockage in carotenoid biosynthetic pathway could divert carbon flux toward the production of lipids and/or other molecules deriving from terpenoid precursors. One characterized albino mutant, namely, strain W4, carries a T-DNA insertion in the *CAR1* gene coding for phytoene desaturase. When cultured in glycerol-containing medium, W4 strain showed significant decreases in cell density and fatty acids content in respect to the wild type strain. Conversely, it reached significantly higher productions of phytoene, CoQ₁₀, and sterols. These were supported by an increased expression of *CAR2* gene that codes for phytoene synthase/lycopene cyclase. Thus, in accordance with the starting hypothesis, the impairment of carotenoids biosynthesis can be explored to pursue the biotechnological exploitation of red yeasts for enhanced production of secondary metabolites with several commercial applications.

Key points

- The production of lipids, carotenoids, and other isoprenoids is tightly interrelated.
- *CAR1* gene mutation results in the overproduction of phytoene, CoQ₁₀, and sterols.
- Albino mutants are promising tools for the production of secondary metabolites.

Keywords Red yeasts · T-DNA insertional mutagenesis · Secondary metabolites · Lipids · Terpenoids

Introduction

The term “red yeasts” indicates a group of species, mainly belonging to the genera *Rhodospiridiobolus*, *Rhodotorula*, and *Sporobolomyces*, that produce pink, orange, or red

colonies, due to the intracellular accumulation of carotenoids (Kot et al. 2019; Mannazzu et al. 2015; Molinè et al. 2012; Urbina and Aime 2018). Besides carotenoids, red yeasts are renowned producers of biomass, enzymes, lipids, biodiesel, fragrances, and biosurfactants (Johnson 2013; Kawahara et al. 2013; Kot et al. 2016; Li et al. 2010; Rubio et al. 2002; Taccari et al. 2012; Tkáčová et al. 2018) and for their ability to convert inexpensive substrates, among which glycerol, industrial by-products and wastewaters, into primary and secondary metabolites of industrial interest, thus reducing the production costs (Cheng and Yang 2016; Cutzu et al. 2013; Ghilardi et al. 2020; Park et al. 2017; Sztokowski et al. 2019).

Based on this evidence, and to pursue their biotechnological exploitation, effective molecular and omic tools were developed for the elucidation of red yeasts metabolic pathways and the management of carbon fluxes (Addis et al.

✉ Ilaria Mannazzu
imannazzu@uniss.it

¹ Institute of Biotechnology, Faculty of Chemical and Food Technology, Slovak University of Technology, Radlinského 9, 812 37 Bratislava, Slovakia

² Department of Agricultural Sciences, Università Degli Studi Di Sassari, Associate Member of the JRU MIRRI-IT, Viale Italia 39, 07100 Sassari, Italy

³ Department of Agricultural, Environmental and Food Sciences, Università Degli Studi del Molise, Via Francesco de Sanctis, 86100 Campobasso, Italy

2016; Bao et al. 2019; Buedenbender et al. 2021; Deligios et al. 2015; Jiao et al. 2019; Landolfo et al. 2018; Li et al. 2020; Liu et al. 2016; Pi et al. 2018; Zhu et al. 2012). T-DNA insertional mutagenesis was used for gene hunting and metabolic engineering in *Rhodospiridium* (now *Rhodotorula*) *toruloides* (Coradetti et al. 2018; Liu et al. 2018) and a high throughput CRISPR/Cas9 system for genome editing was developed (Jiao et al. 2019). More recently, an extensive study of the codon bias was carried out for the optimization of gene sequences for heterologous expression in the red yeasts (Camiolo et al. 2019). Thus, at present, genetically modified red yeast strains are emerging as chassis for enhanced production of carotenoids, lipids, enzymes, and other metabolites (Lin et al. 2017; Wen et al. 2020; Pi et al. 2018; Zhang et al. 2021) that share acetyl-CoA and the mevalonate pathway as common intermediates. In particular, acetyl-CoA is a precursor for the biosynthesis of fatty acids, sterols and other isoprenoids.

Regarding fatty acids biosynthesis, the first step is the carboxylation of acetyl-CoA to malonyl-CoA, catalyzed by acetyl-CoA carboxylase which undergoes feedback regulation by saturated fatty acids. It follows the addition of acetyl-CoA to malonyl-CoA and the subsequent elongation of the resulting molecule catalyzed by the fatty acid synthase complex. Fatty acids are one of the major components of living cells and, besides their essential physiological functions, both fatty acids and their derivatives have several commercial applications for the production of food, soaps, cosmetics, plastics, lubricants, and fuels.

Isoprenoids derive from the condensation of two molecules of acetyl-CoA. This reaction, catalyzed by the enzyme acetoacetyl-CoA synthase, generates acetoacetyl-CoA which enters the mevalonate pathway and originates geranyl pyrophosphate (GPP). The reaction of GPP with isopentenyl pyrophosphate (IPP) produces farnesyl pyrophosphate (FPP) that is the direct precursor of sterols and CoQ. FPP also reacts with IPP to produce geranylgeranyl pyrophosphate (GGPP) that is committed to carotenoid biosynthesis. Thus, FPP is a branch point for the production of carotenoids and other isoprenoids such as sterols and CoQ (Fig. 1). Sterols are important components of cell membranes where they play a role in the regulation of membrane fluidity, in the activity and distribution of integral proteins, and in the control of the cell cycle. Ergosterol serves as a direct precursor for the production of steroidal drugs. Currently, yeast fermentation is the main method for ergosterol production and, by redirecting carbon flux toward ergosterol production, it is possible to enhance ergosterol yields by fungal fermentation (Shang et al. 2006; Liu et al. 2019). In addition, also lanosterol and zymosterol are industrially important being utilized as emulsifiers for cosmetics and precursors to produce cholesterol-lowering substances (Wriessnegger and Pichler 2013). Likewise, coenzyme Q (CoQ), also known as ubiquinone, is commercially important being of great relevance for the cosmetic and healthcare industries (Lee et al. 2017).

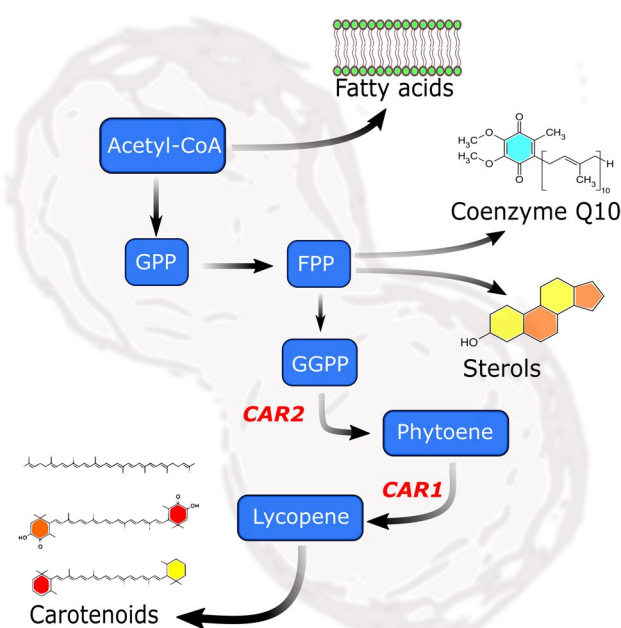


Fig. 1 Biosynthesis of carotenoids, lipids, and other isoprenoids. GPP, geranyl pyrophosphate; FPP, farnesyl pyrophosphate; GGPP, geranylgeranyl pyrophosphate

CoQ, besides being essential in electron transport and oxidative phosphorylation, is a powerful antioxidant that protects cell membranes component from oxidative damage. It consists of a quinone head and an isoprene side chain and, while its chemical synthesis is hampered by several problems among which expensiveness, production of chemical wastes, and lack of stereoselectivity (Lee et al. 2017), its microbial production appears much more feasible. Thus, the biosynthesis of CoQ has been extensively studied in *Saccharomyces cerevisiae*. However, this yeast produces CoQ₆ while, according to Yurkov et al. (2008), red yeasts are a promising source of CoQ₁₀, the one that finds application in human as antioxidant and therapeutic agent.

Here, considering the tight interconnections among carotenoids, fatty acids, sterols, and CoQ metabolic pathways, it was hypothesized that an impairment of carotenogenesis could result in the diversion of carbon flux toward the production of one or more of these metabolites. Based on that, T-DNA insertional mutagenesis was applied to the wild type strain C2.5t1 of *R. mucilaginosa* for the isolation of mutants impaired in carotenoid biosynthesis (albino mutants).

Materials and methods

Strains and media

Rhodotorula mucilaginosa C2.5t1, wild type (WT) strain deposited at the DBVPG Industrial Yeast Collection

(University of Perugia, Italy) with accession number DBVPG 10619 was used in the study. W4 mutant strain is deposited at the Microbial Culture Collection of the University of Sassari, partner of the JRU MIRRI-IT. WT and W4 were maintained on YEPD agar at 4 °C for short-term storage or in YEPGLY40% medium at –80 °C for long-term storage. *Agrobacterium tumefaciens* strain EHA105 contains the binary vector pGI2 in which the nourseothricin resistance-encoding gene (*NAT*) from *Streptomyces noursei* (Krügel et al. 1993) is under the control of the promoter and terminator of the *TUB2* gene of *Rhodotorula graminis* WP1 in the backbone plasmid pPZP-201BK (Abbott et al. 2013).

Yeast culture media and growth conditions were YEPGLY (2% glycerol, 2% peptone, 1% yeast extract); YEPGLY40% (as YEPGLY with 40% glycerol); and YEPD (2% glucose, 2% peptone, 1% yeast extract, 2% agar, when required). Yeast cells were inoculated in 20 mL of YEPGLY medium and incubated at 30 °C, 180 rpm (IKA KS4000ic). After 12 h, yeast cells were transferred into fresh YEPGLY media (50 mL in 250-mL baffled Erlenmeyer flasks) with concentration 1×10^6 cells/mL. Cell growth was carried out at 30 °C under shaking at 180 rpm (IKA KS4000ic) for 72 h during which total cell count, cell dry weight (CDW), and viable cell count were evaluated.

Transformation

Transformation of *R. mucilaginosa* C2.5t1 was carried out according to established protocols for *Agrobacterium tumefaciens*-mediated delivery of DNA (Ianiri et al. 2011; Ianiri and Idnurm 2015). Briefly *R. mucilaginosa* C2.5t1 and *A. tumefaciens* EHA105 co-cultures were incubated on induction medium with 100 or 200 μ M of acetosyringone (AS) (Sigma Aldrich, Italy) (Bundock et al. 1995) for 2 or 3 days prior to transfer to YPD added with three different *NAT* concentrations (100, 150, or 200 μ g/mL) + cefotaxime (200 μ g/mL) (Sigma Aldrich) to inhibit *A. tumefaciens* growth. The *A. tumefaciens* EHA105 strain containing the backbone binary vector pPZP-201BK (containing no gene marker) was used as negative control for transformation.

MIC evaluation

Dose response assays were carried out in 96-well microtiter plates. Briefly, 1×10^6 cells/mL were inoculated in microtiter wells containing 200 μ L YEPD added with increasing concentrations of NaCl (8%, 10%, 12%), H₂O₂ (3 mM, 3.5 mM, 4 mM, 5 mM, 7 mM), and CuSO₄ (15 mM, 17.5 mM, 20 mM, 25 mM, 35 mM, 45 mM).

The microtiter plates were incubated in agitation at 30 °C for 48 h and growth was measured automatically every 30 min at OD600 using a SPECTROstar nano microplate spectrophotometer (BMG Labtech, Ortenberg, Germany). The resulting growth curves were fitted by the primary model of Baranyi and Roberts (1994) wrapped in DMFit Excel Add-in, downloaded from <http://www.combase.cc/index.php/en/tools>, that was utilized also to evaluate the maximum specific growth rate (μ), the duration of lag phase (λ), and the generation time (g). The minimal inhibitory concentration (MIC) was evaluated based on μ values with the “drc” package (v 3.01 Ritz et al. 2015) of the R statistical environment (v 4.0.3—R Core Team (2020). R: A language and environment for statistical computing. R Foundation for Statistical Computing, Vienna, Austria. URL <https://www.R-project.org/>). Results are means \pm standard deviation of three technical replicates of three independent experiments.

General molecular biology procedures

Total DNA extraction was carried out according to Burke et al. (2000). PCR amplifications were carried out in a MyCycler Thermal Cycler (Bio-Rad, Hercules, CA, USA) using HiFidelity Trans Taq with GC-enhancer (TransBi-onovo, Transgen Biotech, Beijing, China). Primers for PCR are reported in Table 1. Agarose gel separations were carried out using 1% (w/v) UltraPure agarose (Invitrogen Life Technologies) with addition of SYBR Safe DNA Gel Stain (Invitrogen Life Technologies) in $1 \times$ TAE (40 mM Tris–acetate and 1 mM EDTA). SharpMass™ 1-kb Ready-to-load DNA Ladder and SharpMass™ 100–100-bp DNA Ladder (EuroClone, Milan, Italy) were utilized as DNA size markers. Gel images were visualized using Chemidoc XRS (Bio-Rad). Purification of DNA from agarose was carried out using Wizard SV gels and PCR Clean-UP

Table 1 Primer pairs utilized

Primer name	Sequence
ai076	5'-AACAGTTGCGCAGCCTGAATG-3'
ai077	5'-AGAGGCGGTTTGCGTATTGG-3'
PhydegF	5'-GCTGACTTCCCACTGCTTC-3'
PhydegR	5'-CCTTGAGGAATCCCAGAAACC-3'
PhySynF	5'-ATGTCTACAAGACGTGCTTCTTGAT-3'
PhySynR	5'-TGACGATAGAGCGACGGTC-3'
CAR1F	5'-CGGTCCCTCGCTCTACCTCA-3'
CAR1R	5'-CCTTGTCGGGAAGACGATG-3'
CAR2F	5'-CCTTCCTCGCCAACGCCTCT-3'
CAR2R	5'-CGTTGTTGGCGTACAGGAGG-3'
ACT1F	5'-CGTTCAGATCCAGGCCGTCT-3'
ACT1R	5'-CGCAATGCAAACCTTCAT-3'

system (Promega, Madison, WI, USA), as indicated by the manufacturer. DNA sequencing was carried out by BMR genomics (University of Padua, Padua, Italy). Inverse PCR (iPCR) was carried out according to Ochman et al. (1988) and Oro et al. (2014) with some modifications. Briefly, *R. mucilaginosa* C2.5t1 genomic DNA was digested with different restriction enzymes that have no recognition sites in the sequence of the PCR product (*XmnI*, *NcoI*, *ClaI*, *XhoI*). After a 3-h incubation at 37 °C, restriction mixtures were heated to 68–90 °C to inactivate the restriction enzymes, and the DNA was ethanol precipitated, diluted in 20 µL, and ligated. The ligation mixtures contained 1–5 ng/µL DNA, 20 U T4 DNA ligase (New England Biolabs), and 1X ligation buffer in 50 µL, and were performed O/N at 4 °C. Each ligation mixture was ethanol precipitated, resuspended in 20 mL H₂O, and subjected to iPCR with primers ai076 and ai077 (Table 1). The inverse PCR mixtures had a final volume of 25 µL and contained 0.5 µM of each primer; 0.2 µM dNTPs; 2.5 µM MgCl₂; 50–100 ng DNA template; and 1 U Taq DNA polymerase in Taq buffer (Transbionovo). The PCR cycling conditions were as follows: initial denaturation at 95 °C for 5 min, followed by 35 cycles of denaturation at 98 °C for 20 s, annealing at 68 °C for 1 min, elongation at 72 °C for 2 min, and final elongation at 72 °C for 10 min. PCR products were visualized on agarose gels and amplicons of interest were purified from agarose and sequenced with primers ai076 and ai077 and PhydegF and PhydegR. DNA sequence data were searched by BLASTn analysis against the genome database. For total RNA extraction, the PureLink RNA Mini Kit (Thermo Fisher Scientific) was utilized according to the manufacturer instructions. The total RNA was treated with DNase (DNase I, Amplification Grade, Thermo Fisher Scientific) for 25 min at room temperature. DNase I was inactivated by adding 2.8 µL 25 mM EDTA and heating for 10 min at 65 °C and total RNA was checked on 1% agarose gel and subjected to PCR amplification using primers ACT1F and ACT1R to assess the presence of residual genomic DNA. RNA quantification was carried out with a Nanodrop (Spectrostar Nano, BMG Labtech) and ~90 ng for each sample underwent retrotranscription with iScript complementary DNA (cDNA) synthesis kit (Bio-Rad) according to the following protocol: 5 min at 25 °C, 30 min at 42 °C, and 5 min at 85 °C. Amplification of cDNA was carried out with primers reported in Table 1 in 10 µL containing: 5 µL master mix (Maxima SYBR Green qPCR Master Mix (2X) Thermo Scientific); 0.3 µL of each primer 10 nM; 1 µL cDNA; and sterile distilled water up to the final volume. The amplification was carried out in a PikoReal 96 Real-Time PCR System (Thermo Scientific). For accurate quantification of the qRT-PCR products, at least three technical replicates of five biological replicates were carried

out. Relative expression was evaluated in respect to actin. Fold changes in expression level of the gene of interest were calculated with the $\Delta\Delta C_t$ method (Vandesompele et al. 2002).

Analytical methods

Total carotenoids content, fatty acids, and lipid structures were evaluated as previously reported Tkáčová et al. (2018). Briefly, lyophilized biomass was directly processed for carotenoids and total lipids extraction according to Folch et al. (1957). After homogenization by a mortar with sea sand, carotenoids were extracted in chloroform/methanol (2:1) mixture for 2 h at room temperature and the mixture was purified by distilled water (1.2 volume of extract). After filtration and centrifugation (3500 rpm, 5 min), the chloroform layer was filtered through anhydrous Na₂SO₄ and evaporated under vacuum. Carotenoids extract was re-suspended in 1 mL of hexane and analyzed by high-performance liquid chromatography (HP 1100, Agilent Technologies) equipped with DAD detector. Ten microliters of carotenoids extract was separated on the column LiChrospher® 100 RP-18 (5 µm) (Merck) with the solvent flow 1 mL/min using a gradient 100% of A (acetonitrile:water:formic acid = 86:10:4 v/v/v) solvent at 0 min, 100% of B (ethyl acetate:formic acid = 96:4 v/v) solvent at 20 min, and 100% of A solvent at 30 min. Carotenoids were identified according to known standards (Sigma, Germany) and evaluated by ChemStation B 01 03 (Agilent technologies).

Fatty acids were analyzed as their methyl esters prepared according to Certik and Shimizu (2000). Lyophilized biomass (10–15 mg) was incubated for 3 h at 50 °C with 1 mL dichloromethane with dissolved 1 mg of heptadecane acid (internal standard, Sigma, USA) to form fatty acid methyl esters (FAME) and 1 mL of distilled water and 1 mL of hexane were added to mixture. Mixture was stirred thoroughly and centrifugated (5000 rpm, 5 min) and FAME were analyzed by gas chromatography GC-6890 N (Agilent Technologies) according to Gajdoš et al. (2015). Chromatograms were evaluated by ChemStation B0103 (Agilent Technologies) and quantified based on retention time of fatty acid standards C4–C24 (Sigma, USA).

Total cellular lipids were analyzed by thin layer chromatography (TLC) on Merck TLC Silica gel 60 plates by CAMAG ATS4 that were scanned by CAMAG TLC Scanner 4 at 400 nm and evaluated by winCATS software ver. 1.4.8 (CAMAG) as described by Gajdoš et al. (2015).

Glycerol content in growth media was evaluated by high-performance liquid chromatography (HPLC) (Agilent Technologies) with UV (210 nm) and RI detectors. Glycerol was separated on the column Aminex HPX-87H using isocratic elution of 5 mM of H₂SO₄ at laboratory

temperature with a flow rate of 0.6 mL/min. Glycerol was identified comparing to known standard. Samples were filtered through a membrane filter (pore size 0.22 μm) before each HPLC analysis.

Results

T-DNA mutagenesis resulted in *CAR1* gene knock out in W4 mutant strain

The transformation protocol utilized for Pucciniomycotina yeasts by Abbott et al. (2013) was here applied to the wild type strain *R. mucilaginosa* C2.5t1 (WT). This protocol is based on the utilization of plasmid pGI2 containing the nourseothricin resistance-encoding gene (*NAT*) from *Streptomyces noursei* (Krügel et al. 1993) as the dominant selection marker, under the control of the promoter and terminator of the *TUB2* gene of *Rhodotorula graminis* WP1. WT transformation, mediated by *Agrobacterium tumefaciens*, allowed the generation of a high number of *R. mucilaginosa* C2.5t1 *NAT*-resistant colonies that were confirmed being transformants by PCR (data not shown). From the selection plates, colonies with the searched albino phenotype could be clearly distinguished, indicating a potential random T-DNA insertion in genes involved in the carotenogenic pathway (Figure S1). A total of 6 *R. mucilaginosa* albino transformants were isolated, and one of these, namely, transformant W4 (Fig. 2), was further characterized. The position of the T-DNA insertion in *R. mucilaginosa* transformant W4 was identified by inverse PCR (IPCR) with primers ai076 and ai077. Amplicon sequencing revealed a T-DNA insertion within the *CAR1* gene coding for phytoene dehydrogenase. Accordingly, when primers PhydeGF and PhydeGR were combined with primers ai076 and ai077 (Fig. 2), two amplicons were obtained thus further confirming the insertion of the *PTUB2-NAT-TTUB2* cassette in *CAR1* gene. Primer pair PhysinF/PhysinR PCR amplified *CAR2* gene coding for phytoene synthase/lycopene cyclase in both strains thus confirming no T-DNA insertion at this level (Fig. 2).

In order to confirm the lack of a functional *CAR1* gene in W4, total RNA was extracted from the mutant and WT strains, reverse transcribed to cDNA, and subjected to RTPCR using primer pairs CAR1F/CAR1R and CAR2F/CAR2R (Landolfo et al. 2018). Results obtained confirmed the lack of *CAR1* and the presence of *CAR2* transcripts in W4 thus supporting the mutation of the *CAR1* gene in this strain (Fig. 2). qRTPCR was also carried out on W4 mutant to evaluate the transcription level of *CAR2* gene. Interestingly, at 24 h W4 mutant showed a 4.2-fold increase in the expression level of *CAR2* gene compared to WT.

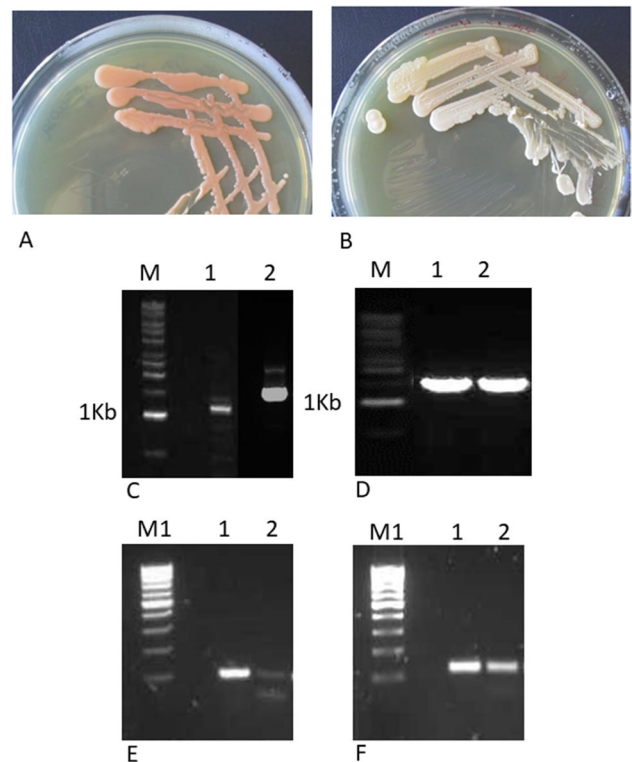


Fig. 2 A Wild type (WT) and B albino mutant W4 on YEPD. C PCR amplification of W4 total DNA with primer pairs PhydegR \times ai77 (lane 1) and PhydegF \times ai76 (lane 2). D PCR amplification of *CAR2* gene on total DNA (lane 1 WT, lane 2 W4). E and F RTPCR with primers CAR1F/CAR1R and CAR2F/CAR2R, respectively (lane 1 WT, lane 2 W4). M, DNA Ladder 1 kb Euroclone; M1, Ladder 100 bp Euroclone

Mutation of the *CAR1* gene impacts cell growth, phytoene production, and stress resistance

To gather information on the phenotypes associated with the *CAR1* mutation, at first the growth kinetics in YEPGLY and glycerol consumption of the WT and W4 strains were analyzed (Fig. 3). WT reached significantly higher cell density as compared to W4 ($p < 0.05$), with the production of 12.23 ± 0.12 g/L DCW and 7.13 ± 0.11 g/L DCW, respectively. Moreover, the two strains differed in the growth kinetics with WT and W4 entering the stationary phase after 48 and 36 h, respectively. Notwithstanding that, growth rate was not significantly different among strains (0.301 ± 0.02 h $^{-1}$ in the WT and 0.405 ± 0.06 h $^{-1}$ in W4). Trends of growth and glycerol utilization were complying. WT completely consumed glycerol after 72 h of cultivation, while at the same time point the W4 strain left 16 g/L residual glycerol thus indicating a negative impact of *CAR1* gene mutation on cell growth on glycerol-containing medium. To assess whether *CAR1* mutation affects stress resistance, both WT and W4 strains were grown in the presence of increasing

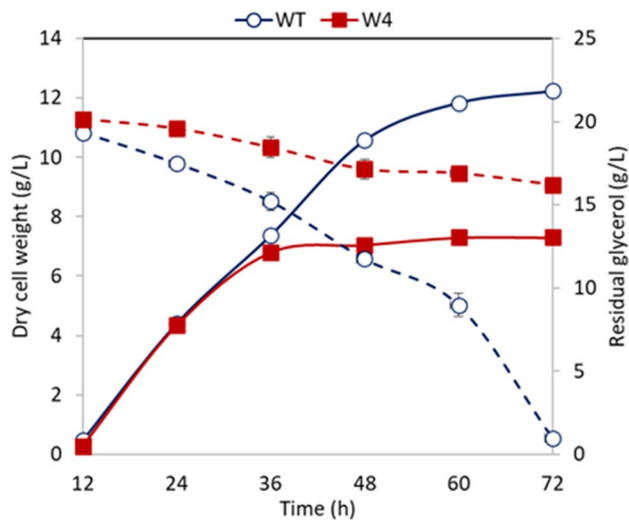


Fig. 3 Growth (continuous lines) and glycerol consumption (dashed lines) in the WT and W4 mutant strains. Results are mean \pm standard deviation of three independent experiments. Where not seen bars lie within the symbols

concentrations of NaCl, CuSO₄, and H₂O₂. As reported in Table 2, W4 showed higher sensitivity to NaCl and CuSO₄, while no differences in H₂O₂ tolerance were observed between the WT and W4 strains.

Regarding total carotenoid production, in the WT strain this peaked in the last day of cultivation (6.18 ± 0.36 mg/L). The main carotenoids were torulene (3.05 ± 0.15 mg/L) and torularhodin (2.04 ± 0.24 mg/L) with lower amounts of γ -carotene (0.53 ± 0.30 mg/L) and β -carotene (0.56 ± 0.07 mg/L), similar to that observed by Moliné et al. (2012) (Figure S2). As expected, no detectable amounts of carotenoids could be observed in W4 mutant. Significant differences were observed also for the intracellular content of phytoene. Phytoene is a colorless carotenoid that is converted to phytofluene, and subsequently to colorful carotenoids, by successive desaturations catalyzed by phytoene desaturase. In accordance with the observed increase in CAR 2 gene expression, W4 mutant accumulated more than twice phytoene content in respect to the WT strain at 24 h (Fig. 4). In both strains, phytoene content decreased at the entry in

Table 2 Minimum inhibitory concentration (MIC) of CuSO₄, H₂O₂, and NaCl

Strain	CuSO ₄ (mM)	H ₂ O ₂ (mM)	NaCl (%)
WT	40.6 ± 3.2^a	3.27 ± 0.5^a	10.18 ± 1.3^a
W4	25.9 ± 2.5^b	3.27 ± 0.6^a	7.74 ± 0.9^b

Results are representative of three technical replicates of three independent experiments. Same superscript letters indicate results not significantly different from WT ($p < 0.05$). Data are means \pm standard deviations from three biological replicates

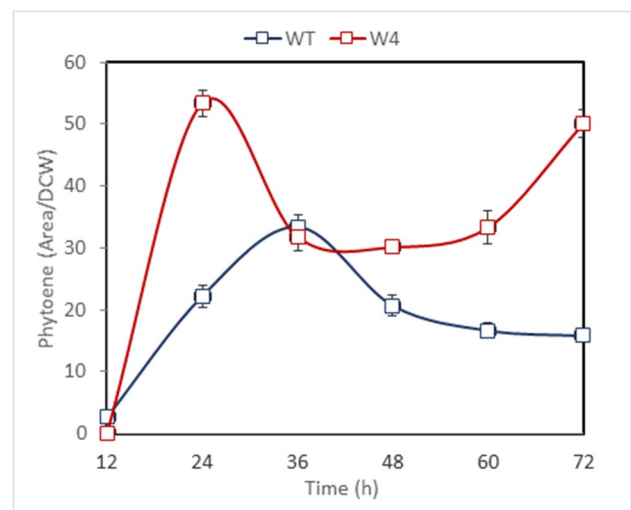


Fig. 4 Phytoene content in the WT and W4 mutant strains. Results are mean \pm standard deviation of three independent experiments. Where not seen bars lie within the symbols

stationary phase. However, while phytoene content declined in the WT strain at the following sampling times, W4 mutant progressively increased it and reached a maximum at 72 h.

CAR1 gene mutation enhances CoQ₁₀ and sterols production

Since phytoene and carotenoids share a common precursor with CoQ₁₀ and sterols (Fig. 1), their content were quantified in the WT and W4 strains. The W4 mutant progressively accumulated CoQ₁₀ till the end of the cultivation process, with a production of 2.9 μ g/L after 72 h of incubation, more than twice compared to the WT (Fig. 5). To assess the production of sterols, squalene and ergosterol were analyzed. Although the two strains showed similar trends of sterols accumulation, the mutant W4 produced significantly higher amounts of squalene and ergosterol ($p < 0.05$) in respect to the WT (Fig. 5), in spite of a lower lipids production at stationary phase (Fig. 6). Sterol esters (SE), categorized as neutral lipids together with TAGs (Czabany et al. 2006; Koch et al. 2014), were continuously produced during the cultivation. The intracellular content of SE, that was significantly lower in W4 strain at the beginning of cultivation, rapidly increased reaching values comparable to that of the WT strain at 24 h (Fig. 7). At the following sampling times, it progressively increased with a trend that was similar to that of the WT although with significantly lower values. In the WT, TAG increased during the exponential phase and remained stable during the stationary phase of growth. On the contrary, W4 showed a progressive decrease in TAG content during stationary phase (Fig. 7). This decline was accompanied by a rise in diacylglycerols (DAG) and free

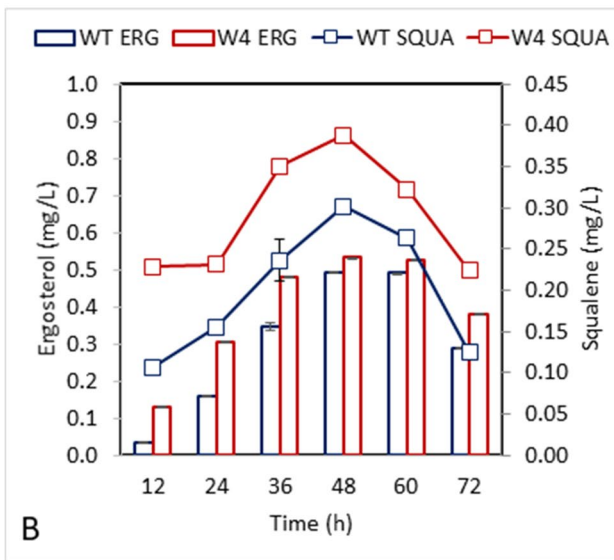
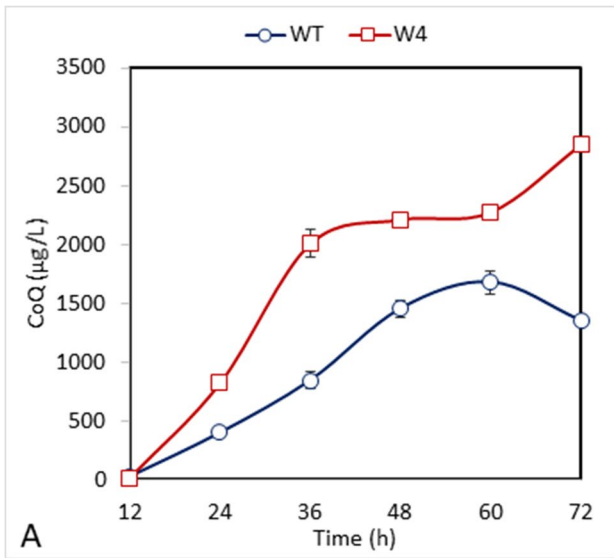


Fig. 5 CoQ₁₀ (A) and sterol content (B) in the WT and W4 mutant strains. Results are mean ± standard deviation of three independent experiments. Where not seen bars lie within the symbols

fatty acids, possibly due to lipase-mediated TAG degradation (Kohlwein 2010) (Figure S3).

CAR1 gene mutation results in a decrease in fatty acids content and a variation in fatty acids composition

Since carotenoids and fatty acids share acetyl-CoA as a common precursor, the amount and composition of total fatty acids (TFA) were analyzed in the WT and W4 strains. Indeed, in the WT strain the production of TFA was rather low in respect to that expected in the oleaginous species *R. mucilaginosa* (Rani et al. 2013). In this strain, TFA

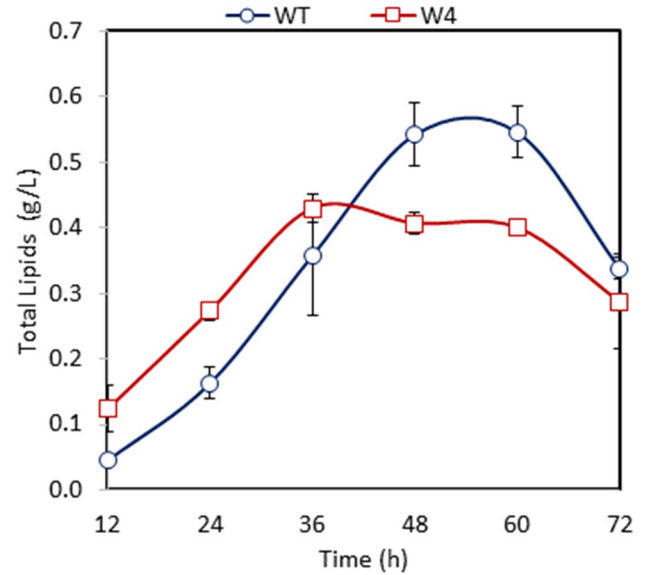


Fig. 6 Total lipid content in the WT and W4 mutant strains. Results are mean ± standard deviation of three independent experiments. Where not seen bars lie within the symbols

productivity reached its maximum at stationary phase (about 1.0 g/L), when total fatty acids represented about 9% of DCW (Fig. 8). W4 showed significantly lower production of TFA compared to the WT strain ($p < 0.05$), with a maximum of about 0.4 g/L, accounting roughly for 4–5% of DCW. To evaluate whether these differences in TFA production could reflect also differences in fatty acids composition, the fatty acids (FA) profiles of WT and W4 were determined (Figure S4). In WT, oleic acid (OA) content increased during exponential phase and declined during stationary phase. This trend was accompanied by significant ($p < 0.05$) increases in linoleic acid (LA) (from 11% at 48 h to 32% at 72 h) and by the doubling of linolenic acid (ALA) (from 2% at 48 h to 4% at 72 h). Indeed, the kinetics of accumulation of OA showed opposite trend in respect to that of LA and ALA. Also, in W4 the main fatty acid was OA. However, in this case, OA content, after reaching its maximum at 36 h, showed no major variations at the following sampling times. Accordingly, LA and ALA percentages showed a progressive decrease from 12 to 36 h and no subsequent variations (Figure S4).

Discussion

CAR1 gene encodes a phytoene desaturase (Car1p) that catalyzes the sequential desaturation of phytoene and leads to the production of lycopene, in turn converted in torulene, torularhodin, and β-carotene. Phytoene is a colorless carotenoid and together with phytofluene, is a rarity within the

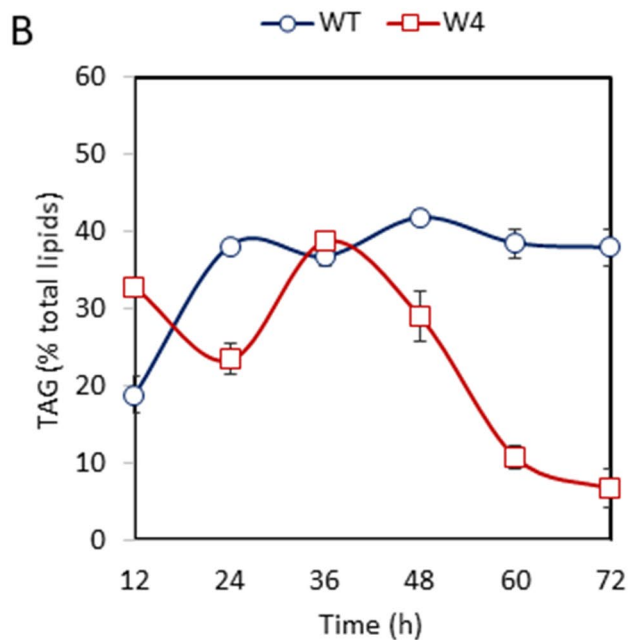
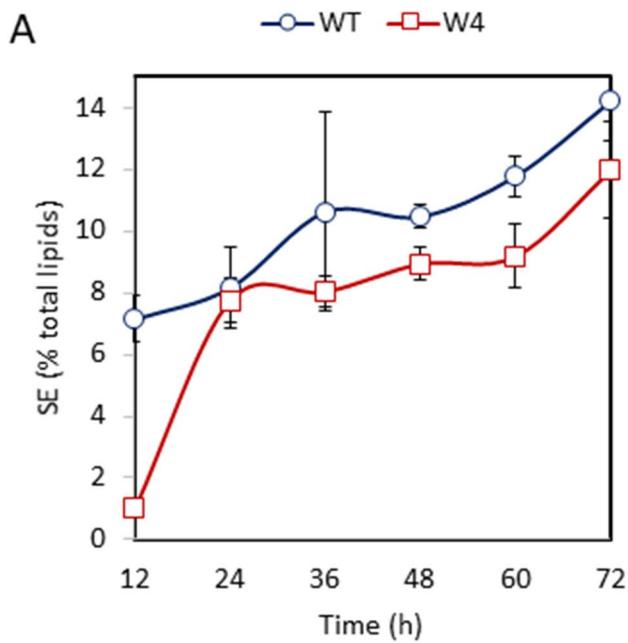


Fig. 7 Sterol esters (A) and triacylglycerol (B) in the WT and W4 mutant strains. Results are mean \pm standard deviation of three independent experiments. Where not seen bars lie within the symbols

“Carotenoid Kingdom” (Melendez-Martinez et al. 2015). Although being less characterized than pigmented carotenoids, it has been described as a powerful free radical scavenger due to its absorption maxima in the UV region (Martinez et al. 2014; Melendez-Martinez et al. 2018).

The accumulation of phytoene was not expected in WT strain while it was rather probable in W4. In accordance with this hypothesis, the decline in phytoene content observed

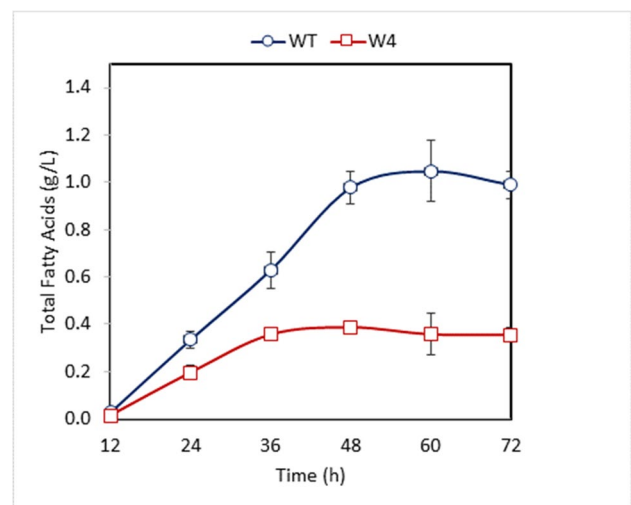


Fig. 8 Fatty acids content in the WT and W4 mutant strains. Results are mean \pm standard deviation of three independent experiments. Where not seen bars lie within the symbols

in WT during the stationary phase of growth was due to the activity of Car1p and resulted in the intracellular accumulation of carotenoids. On the contrary, the progressive accumulation of phytoene obtained in W4, lacking detectable amounts of carotenoids, was the result of the lack of a functional Car1p and was compatible with the increase in *CAR2* gene expression. Car2p catalyzes the production of phytoene from the condensation of two molecules of geranylgeranyl pyrophosphate (Fraser and Bramley 2004) and is considered as the most important regulatory enzyme in carotenoid biosynthesis. In carrots, carotenoids proved to modulate phytoene synthase/lycopene cyclase protein level through a posttranscriptional feedback mechanism (Arango et al. 2014). Here, the increase in the transcription levels of *CAR2* gene in W4 is compatible with the hypothesis that carotenoids control the transcription level of *CAR2* gene through a negative feedback mechanism.

Similar to that observed for phytoene, *CAR1* mutation resulted in the enhancement of CoQ₁₀ and sterol content. In the WT strain, that relies on a functional carotenoid pathway, FPP was expected to be available for CoQ₁₀ and sterols formation, but also for the production of GGPP, phytoene and, in cascade, pigmented carotenoids. On the contrary, CoQ₁₀ and sterols accumulation in W4 strain was a plausible consequence of the diversion of FPP toward the production of other isoprenoids. Indeed, the observed overproduction of phytoene, CoQ₁₀, and sterols, besides being the consequence of the impairment of carotenoid biosynthesis, could represent also a cellular strategy to increase membrane stabilization and stress tolerance in the absence of carotenoids. Results obtained with H₂O₂ seem compatible with this hypothesis since the two strains showed the same

tolerance to this prooxidant and confirm that carotenoids are not crucial for H₂O₂ resistance (Landolfo et al. 2019). On the contrary, the decrease in NaCl and CuSO₄ MICs in W4 mutant strain suggests that carotenoids mediate the cellular response to these two stressors. Indeed, the two strains differed also in TFA content and in the kinetics of OA, LA, and ALA accumulation. In particular, in the WT strain, the stationary phase increase in LA and ALA was possibly due to OA desaturation catalyzed by $\Delta 12$ - and $\Delta 15$ -desaturases (Koch et al. 2014; Tsakraklides et al. 2018) and/or to fatty acids β -oxidation occurring when acetyl-CoA is needed as a crucial substrate for the production of secondary metabolites (Tkáčová et al. 2018). Since FA are building blocks for cellular membranes and a source of cellular energy, these variations could be, at least in part, responsible for the reduction of biomass production in glycerol-containing medium and the decreased tolerance to NaCl and CuSO₄ observed in W4 mutant strain.

The two strains differed also for the kinetics of accumulation of sterol esters (SE) and triacylglycerols (TAG). These are neutral lipids that serve as lipid storage and secondary energy source and are important for the maintenance of cellular homeostasis also in response to stressful growth conditions (Rani et al. 2013; Koch et al. 2014; Tsakraklides et al. 2018). In particular, SE and TAG are produced when the synthesis of sterols and TFA exceeds the cellular requirements, to counteract their toxic effect. SE are synthesized via acyl-CoA-dependent esterification catalyzed by the two acyl-CoA:sterol acetyltransferases Are1p and Are2p (Czabany et al. 2006; Koch et al. 2014; Graef 2018). TAG derive from the esterification of glycerol with three molecules of fatty acids. This is accomplished through diacyl-glycerol (DAG), which is a common precursor for TAG and phospholipids biosynthesis (Handee et al. 2016). Thus, the production of higher SE amounts in W4, in spite of the lower TFA and total lipids content in stationary phase, is in accordance with the overproduction of sterols by W4 and with mevalonate and isoprenoid pathways being pushed toward sterol synthesis as a result of the impairment of carotenoids biosynthesis caused by *CARI* mutation. On the contrary, the decline of TAG and the concomitant increase of DAG in W4 mutant seem compatible with the need to recruit phospholipids for membrane synthesis during the stationary phase of growth. In accordance with that reported by Handee et al. (2016), TAG hydrolysis is not needed in the WT strain where fatty acids can be synthesized by de novo activities.

In summary, according to the hypothesis that an impairment of carotenoid biosynthesis may redirect carbon flux toward the production of lipids and isoprenoids, here, the mutation of *CARI* gene determined significant increases in the production of phytoene, CoQ₁₀, and sterols. All these are high-value secondary metabolites with recognized application in the pharmaceutical and the cosmetics industries. The

ability of red yeasts to convert inexpensive substrates into biomass enriched in valuable metabolites represents an extra advantage for a sustainable production of these goods at the industrial scale.

Supplementary Information The online version contains supplementary material available at <https://doi.org/10.1007/s00253-021-11673-5>.

Acknowledgements The JRU MIRRI-IT (<http://www.mirri-it.it/>) is greatly acknowledged for scientific support.

Author contribution IM, GI, and MC conceived and designed research. JT and GI conducted experiments. RC and MC contributed new reagents or analytical tools. GZ and IM analyzed data. IM and JT wrote the manuscript. All authors read and approved the manuscript.

Funding This work was supported by Slovak Ministry of Education, Science, Research and Sport “VEGA 1/0323/19” (P.I. M.C.) and by University of Sassari, “Fondo di Ateneo per la Ricerca 2020,” (P.I. I.M.). GZ gratefully acknowledges Sardinia Regional Government for the financial support of his research grant (Regional Operational Program of the European Social Fund (ROP ESF) 2014–2020-C.U.P. J86C18000270002). JT was financially supported by COST CA15136 EUROCARTEN. GI and RC are supported by the PON AIM Program Azione I.2 “Attrazione e Mobilità dei Ricercatori”.

Data availability All data generated or analyzed during this study are included in this published article (and its supplementary information files).

Code availability Not applicable.

Declarations

Ethics approval This article does not contain any studies with human participants or animals performed by any of the authors.

Conflict of interest The authors declare no competing interests.

References

- Abbott EP, Ianiri G, Castoria R, Idnurm A (2013) Overcoming recalcitrant transformation and gene manipulation in Pucciniomycotina yeasts. *Appl Microbiol Biotechnol* 97:283–295
- Addis MF, Tanca A, Landolfo S, Abbondio M, Cutzu R, Biosa G, Pagnozzi D, Uzzau S, Mannazzu I (2016) Proteomic analysis of *Rhodotorula mucilaginosa*: dealing with the issues of a non-conventional yeast. *Yeast* 33:433–449
- Arango J, Jourdan M, Geoffriau E, Beyer P, Welsch R (2014) Carotene hydroxylase activity determines the levels of both α -carotene and total carotenoids in orange carrots. *Plant Cell* 26(5):2223–2233
- Bao R, Gao N, Lv J, Ji C, Liang H, Li S, Yu L, Wang Z, Lin X (2019) Enhancement of torularhodin production in *Rhodospiridium torulooides* by *Agrobacterium tumefaciens*-mediated transformation and culture condition optimization. *J Agric Food Chem* 4:1156–1164
- Baranyi J, Roberts TA (1994) A dynamic approach to predicting bacterial growth in food. *Int J Food Microbiol* 23(3–4):277–294
- Buedenbender L, Kumar A, Blümel M, Kempken F, Tasdemir D (2021) Genomics- and metabolomics-based investigation of the deep-sea

- sediment-derived yeast, *Rhodotorula mucilaginosa* 50–3-19/20B. *Mar Drugs* 19:14. <https://doi.org/10.3390/md19010014>
- Bundock P, den Dulk-Ras A, Beijersbergen A, Hooykaas PJJ (1995) Trans-kingdom T-DNA transfer from *Agrobacterium tumefaciens* to *Saccharomyces cerevisiae*. *EMBO J* 14(13):3206–3214
- Burke D, Dean D, Tim S (2000). *Methods in yeast genetics 2000: a Cold Spring Harbor laboratory course manual*. Cold Spring Harbor Press, New York.
- Camiolo S, Toome-Heller M, Aime MC, Haridas S, Grigoriev IV, Porceddu A, Mannazzu I (2019) An analysis of codon bias in six red yeasts species. *Yeast* 36(1):53–64. <https://doi.org/10.1002/yea.3359>
- Certik M, Shimizu S (2000) Kinetic analysis of oil biosynthesis by an arachidonic acid-producing fungus, *Mortierella alpina* 1S–4. *Appl Microbiol Biotechnol* 54:224–230
- Cheng YT, Yang CF (2016) Using strain *Rhodotorula mucilaginosa* to produce carotenoids using food wastes. *J Taiwan Inst Chem Eng* 61:270–275
- Coradetti ST, Pinel D, Geiselman GM, Ito M, Mondo SJ, Reilly MC, Cheng YF, Bauer S, Grigoriev IV, Gladden JM, Simmons BA, Brem RB, Arkin AP, Skerker JM (2018) Functional genomics of lipid metabolism in the oleaginous yeast *Rhodospiridium toruloides*. *eLife* 7:e32110. <https://doi.org/10.7554/eLife.32110>
- Cutzu R, Coi A, Rosso F, Bardi L, Ciani M, Budroni M, Zara G, Zara S, Mannazzu I (2013) From crude glycerol to carotenoids by using a *Rhodotorula glutinis* mutant. *World J Microbiol Biotechnol* 29:1009–1017. <https://doi.org/10.1007/s11274-013-1264-x>
- Czabany T, Athenstaedt K, Daum G (2006) Synthesis, storage and degradation of neutral lipids in yeast. *Biochim Biophys Acta* 1771:299–309. <https://doi.org/10.1016/j.bbaliip.2006.07.001>
- Deligios M, Fraumene C, Abbondio M, Mannazzu I, Tanca A, Addis MF, Uzzau S (2015) Draft genome sequence of *Rhodotorula mucilaginosa*, an emergent opportunistic pathogen. *Genome Announc* 3(2):e00201–e215. <https://doi.org/10.1128/genomeA.00201-15>
- Folch J, Lees M, Sloane-Stanley GH (1957) A simple method for the isolation and purification of total lipids from animal tissues. *J Biol Chem* 226:497–509
- Fraser PD, Bramley PM (2004) The biosynthesis and nutritional uses of carotenoids. *Prog Lipid Res* 43:228–265
- Gajdoš P, Nicaud JM, Rossignol T, Čertík M (2015) Single cell oil production on molasses by *Yarrowia lipolytica* strains overexpressing DGA2 in multicopy. *Appl Microbiol Biotechnol* 99:8065–8074
- Ghilardi C, Negrete PS, Carelli AA, Boroni V (2020) Evaluation of olive mill waste as substrate for carotenoid production by *Rhodotorula mucilaginosa*. *Bioresour Bioprocess* 7:52
- Graef M (2018) Lipid droplet-mediated lipid and protein homeostasis in budding yeast. *FEBS Lett* 592:1291–1303
- Handee W, Li X, Hall KW, Deng X, Li F, Benning C, Williams BL, Kuo MH (2016) An energy independent pro-longevity function of triacylglycerol in yeast. *PLOS Genet* 12(2):e1005878
- Ianiri G, Wright SAI, Castoria R, Idnurm A (2011) Development of resources for the analysis of gene function in Pucciniomycotina red yeasts. *Fungal Genet Biol* 48:685–695
- Ianiri G, Idnurm A (2015) Essential gene discovery in the basidiomycete *Cryptococcus neoformans* for antifungal drug target prioritization. *mBio*. 6(2):e02334
- Jiao X, Zhang Y, Liu X, Zhang Q, Zhang S, Zhao ZK (2019) Developing a CRISPR/Cas9 system for genome editing in the basidiomycetous yeast *Rhodospiridium toruloides*. *Biotechnol J* 14(7):e1900036. <https://doi.org/10.1002/biot.201900036>
- Johnson EA (2013) Biotechnology of non-*Saccharomyces* yeasts—the basidiomycetes. *Appl Microbiol Biotechnol* 97:7563–7577
- Kawahara H, Hirai A, Minabe T, Obata H (2013) Stabilization of astaxanthin by a novel biosurfactant produced by *Rhodotorula mucilaginosa* KUGPP-1. *Biocontrol Sci* 18:21–28
- Koch B, Schmidt C, Daum G (2014) Storage lipids of yeasts: a survey of nonpolar lipid metabolism in *Saccharomyces cerevisiae*, *Pichia pastoris*, and *Yarrowia lipolytica*. *FEMS Microbiol Rev* 38(5):892–915. <https://doi.org/10.1111/1574-6976.12069>
- Kohlwein SD (2010) Triacylglycerol homeostasis: insights from yeast. *J Biol Chem* 285:15663–15667
- Kot AM, Blazejak S, Kurcz A, Gientka I, Kieliszek M (2016) *Rhodotorula glutinis* potential source of lipid, carotenoids, and enzymes for use in industries. *Appl Microbiol Biotechnol* 100:6103–6117
- Kot AM, Błażejak S, Kieliszek M, Gientka I, Bryś J (2019) Simultaneous production of lipids and carotenoids by the red yeast *Rhodotorula* from waste glycerol fraction and potato wastewater. *Appl Biochem Biotech* 189:589–607
- Krügel H, Fiedler G, Smith C, Baumberg S (1993) Sequence and transcriptional analysis of the nourseothricin acetyltransferase-encoding gene nat1 from *Streptomyces noursei*. *Gene* 127(1):127–131. [https://doi.org/10.1016/0378-1119\(93\)90627-f](https://doi.org/10.1016/0378-1119(93)90627-f)
- Landolfo S, Ianiri G, Camiolo S, Porceddu A, Mulas G, Chessa R, Zara G, Mannazzu I (2018) CAR gene cluster and transcript levels of carotenogenic genes in *Rhodotorula mucilaginosa*. *Microbiology* 164(1):78–87. <https://doi.org/10.1099/mic.0.000588>
- Landolfo S, Chessa R, Zara G, Zara S, Budroni M, Mannazzu I (2019) *Rhodotorula mucilaginosa* C2.5t1 modulates carotenoid content and CAR genes transcript levels to counteract the pro-oxidant effect of hydrogen peroxide. *Microorganisms* 7(9):316. <https://doi.org/10.3390/microorganisms7090316>
- Lee SQE, Tan TS, Kawamukai M, Chen ES (2017) Cellular factories for coenzyme Q10 production. *Microb Cell Fact* 16:39. <https://doi.org/10.1186/s12934-017-0646-4>
- Li CJ, Zhao D, Cheng P, Zheng L, Yu G-H (2020) Genomics and lipidomics analysis of the biotechnologically important oleaginous red yeast *Rhodotorula glutinis* ZHK provides new insights into its lipid and carotenoid metabolism. *BMC Genomics* 21(1):834. <https://doi.org/10.1186/s12864-020-07244-z>
- Li M, Liu GL, Chi Z, Chi Z-M (2010) Single cell oil production from hydrolysate of cassava starch by marine-derived yeast *Rhodotorula mucilaginosa* TJY15a. *Biomass Bioen* 34:101–107. <https://doi.org/10.1016/j.biombioe.2009.10.005>
- Lin X, Gao N, Liu S, Zhang S, Song S, Dong X, Su Y, Zhao ZK, Zhu B (2017) Characterization the carotenoid productions and profiles of three *Rhodospiridium toruloides* mutants from *Agrobacterium tumefaciens*-mediated transformation. *Yeast* 34:335–342
- Liu J-F, Xia J-J, Nie K-L, Wang F, Deng L (2019) Outline of the biosynthesis and regulation of ergosterol in yeast. *World J Microbiol Biotechnol* 35:98. <https://doi.org/10.1007/s11274-019-2673-2>
- Liu Y, Koh CMJ, Yap SA, Du M, Myntzu M, Ji L (2018) Identification of novel genes in the carotenogenic and oleaginous yeast *Rhodotorula toruloides* through genome wide insertional mutagenesis. *BMC Microbiol* 18:14. <https://doi.org/10.1186/s12866-018-1151-6>
- Liu Y, Yap SA, Koh CMJ, Ji L (2016) Developing a set of strong intronic promoters for robust metabolic engineering in oleaginous *Rhodotorula* (*Rhodospiridium*) yeast species. *Microb Cell Fact* 15(1):200. <https://doi.org/10.1186/s12934-016-0600-x>
- Mannazzu I, Landolfo S, Lopes da Silva T, Buzzini P (2015) Red yeasts and carotenoids production: outlining a future for non-conventional yeasts of biotechnological interest. *World J Microbiol Biotechnol* 31:1665–1673
- Martinez A, Stinco CM, Melendez-Martinez AJ (2014) Free radical scavenging properties of phytofluene and phytoene isomers as compared to lycopene: a combined experimental and theoretical study. *J Phys Chem* 118(33):9819–9825
- Melendez-Martinez A, Mapelli-Brahm P, Benitez-Gonzalez A, Stinco CM (2015) A comprehensive review on the colorless carotenoid phytoene and phytofluene. *Arch Biochem Biophys* 572:88–200

- Melendez-Martinez A, Mapelli-Brahm P, Stinco CM (2018) The colourless carotenoids phytoene and phytofluene: from dietary sources to their usefulness for the functional foods and nutraceuticals industries. *J Food Comp Analysis* 67:91–103
- Moliné M, Libkind D, van M (2012) Production of torularhodin, torulene, and β -carotene by *Rhodotorula* yeasts. *Methods Mol Biol* 898:275–83.
- Ochman H, Gerber AS, Hartl L (1988) Genetic application of an inverse polymerase chain reaction. *Genetics* 120:621–623
- Oro L, Zara S, Fancellu F, Mannazzu I, Budroni M, Ciani M, Comitini F (2014) TpBGL2 codes for a *Tetrapisispora phaffii* killer toxin active against wine spoilage yeasts. *FEMS Yeast Res* 14:464–471
- Park GW, Chang HN, Jung K, Seo C, Kim YC, Choi JH, Woo HC, Hwang IJ (2017) Production of microbial lipid by *Cryptococcus curvatus* on rice straw hydrolysates. *Process Biochem* 56:147–153. <https://doi.org/10.1016/j.procbio.2017.02.0>
- Pi H-W, Anandharaj W, Kao Y-Y, Lin Y-J, Chang J-J, Li W-H (2018) Engineering the oleaginous red yeast *Rhodotorula glutinis* for simultaneous β -carotene and cellulase production. *Sci Rep* 8:10850
- Rani SH, Saha S, Rajasekharan R (2013) A soluble diacylglycerol acyltransferase is involved in triacylglycerol biosynthesis in the oleaginous yeast *Rhodotorula glutinis*. *Microbiology* 159:155–166
- Rubio MC, Runco R, Navarro AR (2002) Invertase from a strain of *Rhodotorula glutinis*. *Phytochemistry* 61:605–609. [https://doi.org/10.1016/S0031-9422\(02\)00336-9](https://doi.org/10.1016/S0031-9422(02)00336-9)
- Shang F, Wen S, Wang X, Tan T (2006) High-cell-density fermentation for ergosterol production by *Saccharomyces cerevisiae*. *J Biosci Bioeng* 101(1):38–41
- Szotkowski M, Byrtusova D, Haronikova A, Vysoka M, Rapta M, Shapaval V, Marova I (2019) Study of metabolic adaptation of red yeasts to waste animal fat substrate. *Microorganisms* 7:578
- Taccari M, Canonico L, Comitini F, Mannazzu I, Ciani M (2012) Screening of yeasts for growth on crude glycerol and optimization of biomass production. *Bioresour Technol* 110:488–495
- Tkáčová J, Klempová T, Čertík M (2018) Kinetic study of growth, lipid and carotenoid formation in β -carotene producing *Rhodotorula glutinis*. *Chem Papers* 72:1193–1203
- Tsakraklides V, Kamineni A, Consiglio AL, MacEwen K, Friedlander J, Blitzblau HG, Hamilton MA, Crabtree DV, Su A, Afshar J, Sullivan JE, LaTouf WG, South CR, Greenhagen EH, Shaw AJ, Brevnova EE (2018) High-oleate yeast oil without polyunsaturated fatty acids. *Biotechnol Biofuels* 11:131
- Urbina H, Aime MC (2018) A closer look at Sporidiobolales: ubiquitous microbial community members of plant and food biospheres. *Mycologia* 110(1):79–92. <https://doi.org/10.1080/00275514.2018.1438020>
- Vandesompele J, De Preter K, Pattyn F, Poppe B, Van Roy N, De Paepe A, Speleman F (2002) Accurate normalisation of real-time quantitative RT-PCR data by geometric averaging of multiple internal control genes. *Gen Biol* 3:1–12
- Wen Z, Zhang S, Odoh CK, Jin M, Zhao ZK (2020) *Rhodospiridium toruloides* - a potential red yeast chassis for lipids and beyond. *FEMS Yeast Res* 20(5):foaa038. <https://doi.org/10.1093/femsyr/foaa038>.
- Wriessnegger T, Pichler H (2013) Yeast metabolic engineering—targeting sterol metabolism and terpenoid formation. *Prog Lipid Res* 52(3):277–293
- Yurkov AM, Vustin MM, Tyaglov BV, Maksimova IA, Sineokiy SP (2008) Pigmented basidiomycetous yeasts are a promising source of carotenoid and ubiquinone Q10. *Microbiology* 77(1):5–10
- Zara G, Farbo MG, Multineddu C, Migheli Q, Budroni M, Zara S, Mannazzu I (2021) Exploring the biodiversity of red yeasts for in vitro and in vivo phenotypes relevant to agri-food-related processes. *Fermentation* 7:2. <https://doi.org/10.3390/fermentation7010002>
- Zhang Y, Peng J, Zhao H, Shi S (2021) Engineering oleaginous yeast *Rhodotorula toruloides* for overproduction of fatty acid ethyl esters. *Biotechnol Biofuels* 14(1):115. <https://doi.org/10.1186/s13068-021-01965-3>
- Zhu Z, Zhang S, Liu H, Shen H, Lin X, Yang F, Zhou YJ, Jin G, Ye M, Zou H, Zhao ZK (2012) A multi-omic map of the lipid-producing yeast *Rhodospiridium toruloides*. *Nat Commun* 3:1112. <https://doi.org/10.1038/ncomms2112>

Publisher's note Springer Nature remains neutral with regard to jurisdictional claims in published maps and institutional affiliations.